

Mesenchymal Stem Cells Provide Better Results Than Hematopoietic Precursors for the Treatment of Myocardial Infarction

Ana Armiñán, PhD,*† Carolina Gandía, PhD,*† J. Manuel García-Verdugo, PhD,†‡
Elisa Lledó, PhD,*† César Trigueros, PhD,§ Amparo Ruiz-Saurí, MD, PhD,‡
María Dolores Miñana, PhD,|| Pilar Solves, MD, PhD,¶ Rafael Payá, MD, PhD,||
J. Anastasio Montero, MD, PhD,*† Pilar Sepúlveda, PhD*†

Valencia and San Sebastián, Spain

Objectives	The purpose of this study was to compare the ability of human CD34 ⁺ hematopoietic stem cells and bone marrow mesenchymal stem cells (MSC) to treat myocardial infarction (MI) in a model of permanent left descendent coronary artery (LDA) ligation in nude rats.
Background	Transplantation of human CD34 ⁺ cells and MSC has been proved to be effective in treating MI, but no comparative studies have been performed to elucidate which treatment prevents left ventricular (LV) remodelling more efficiently.
Methods	Human bone marrow MSC or freshly isolated CD34 ⁺ cells from umbilical cord blood were injected intramyocardially in infarcted nude rats. Cardiac function was analyzed by echocardiography. Ventricular remodelling was evaluated by tissue histology and electron microscopy, and neo-formed vessels were quantified by immunohistochemistry. Chronic local inflammatory infiltrates were evaluated in LV wall by hematoxylin-eosin staining. Apoptosis of infarcted tissue was evaluated by terminal deoxynucleotidyl transferase dUTP nick end labeling assay.
Results	Both cell types induced an improvement in LV cardiac function and increased tissue cell proliferation in myocardial tissue and neoangiogenesis. However, MSC were more effective for the reduction of infarct size and prevention of ventricular remodelling. Scar tissue was $17.48 \pm 1.29\%$ in the CD34 group and $10.36 \pm 1.07\%$ in the MSC group ($p < 0.001$ in MSC vs. CD34). Moreover, unlike MSC, CD34 ⁺ -treated animals showed local inflammatory infiltrates in LV wall that persisted 4 weeks after transplantation.
Conclusions	Mesenchymal stem cells might be more effective than CD34 ⁺ cells for the healing of the infarct. This study contributes to elucidate the mechanisms by which these cell types operate in the course of MI treatment. (J Am Coll Cardiol 2010;55:2244–53) © 2010 by the American College of Cardiology Foundation

Myocardial infarction (MI) is still one of the main causes of mortality and morbidity in developed countries. In the acute setting, approaches to improve myocardial perfusion range from pharmacological therapies (thrombolysis) to mechanical procedures (primary angioplasty). Recently, several stem cell types have been used in small and large clinical trials in

adjunction to conventional therapies for the treatment of MI. First studies of cellular angioplasty were held with bone marrow mononuclear cells (1), and to date all clinical trials have reported similar results, with approximately 8% improvement in global left ventricular (LV) fraction, reduced end-systolic volumes, and improved perfusion in the infarcted area 4 to 6 months after cell transplantation (2,3).

See page 2254

From the *Fundación para la Investigación Hospital Universitario La Fe, Valencia, Spain; †Centro de Investigación Príncipe Felipe, Valencia, Spain; ‡Universidad de Valencia, Valencia, Spain; §Fundación Inbiomed, San Sebastián, Spain; ||Hospital General Universitario de Valencia, Valencia, Spain; and the ¶Centro de Transfusiones de la Comunidad Valenciana, Valencia, Spain. This work was supported by grants from the Instituto de Salud Carlos III for the Regenerative Medicine Program of Valencian Community to Centro de Investigación Príncipe Felipe and from the FIS (PI04/2366, PI07/784, and CP08/80). Dr. Sepúlveda acknowledges support from Miguel Servet and RETICS programs (Instituto de Salud Carlos III).

Manuscript received July 5, 2009; revised manuscript received July 31, 2009, accepted August 10, 2009.

These clinical trials were followed by others with cellular samples enriched for cell progenitors, like circulating blood progenitor cells (2,4) or bone marrow mesenchymal stem cells (MSC) (5,6). However, the enormous variability in the technical procedures used in each study made comparison difficult. For this reason, studies using dif-

ferent cell types in similar conditions will move the field forward.

In this study, we designed a set of experiments to compare, head-to-head, the ability of 2 human adult stem cell populations—CD34⁺ cells and MSC—to repair MI. These cell types have become the most clinically relevant for cardiovascular cell therapies. Thus, the data presented here could be useful for the design of more efficient clinical trials with less collateral effects.

Methods

All procedures were approved by the Instituto de Salud Carlos III and institutional ethical and animal care committees.

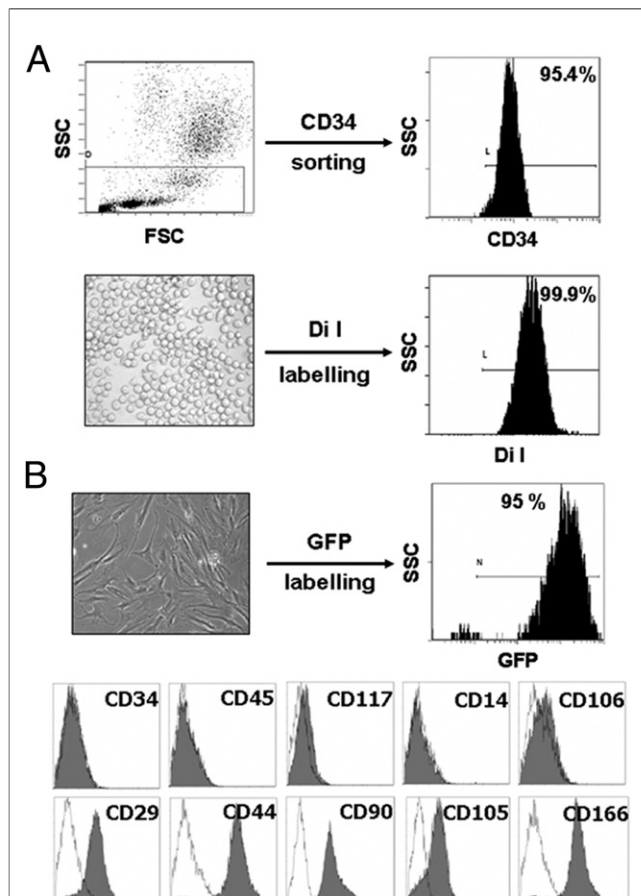


Figure 1 Characterization of Human CD34⁺-Umbilical Cord Blood Cells and Bone Marrow MSC

(A) Cell sorting of umbilical cord blood mononuclear fraction with the MACS system (Miltenyi, Bergisch, Germany) and labeling of freshly isolated CD34⁺ cells with the vital marker DiI (Molecular Probes, Invitrogen, Eugene, Oregon). Isolated CD34⁺ cells were photographed at 160× magnification. (B) Mesenchymal stem cells (MSC) in culture (magnification 200×). Retroviral labeling of cultured MSC yielded 95% infection as detected by flow cytometric analysis of green fluorescent protein (GFP)-MSC. Representative flow cytometric analysis of antigenic expression is shown. **Shaded histograms** represent staining with specific antibodies, and **open histograms** correspond to matched isotypes. FSC = forward scatter; SSC = side scatter.

Cells, culture conditions, and retroviral labeling. Human bone marrow MSC (n = 3) (Inbiomed, San Sebastian, Guipuzcoa, Spain) were cultured following the manufacturers' instructions and retrovirally labeled with green fluorescent protein as previously reported (7). Transduction efficiency was evaluated by flow cytometry. The CD34⁺ human umbilical cord blood cells (n = 14) were isolated with the autoMACS system (Miltenyi, Bergisch, Germany) as previously reported (8). For some experiments CD34⁺ cells were labeled with the vital marker CM-Di I, following the manufacturers' instructions (Molecular Probes, Invitrogen, Eugene, Oregon).

Animals. Nude rats weighing 200 to 250 g (HIH-Foxn1^{rnu}, Charles River Laboratories, Inc., Wilmington, Massachusetts) were used. The initial number of animals included in the study was 90. Animals with fractional shortening (FS) above 35% after MI were excluded. Mortality in all groups due to surgical procedures was approximately 30%. **MI and cell transplantation.** Permanent ligation of the left coronary artery was performed as previously described (7,9). Seven days later, rats were anesthetized with sevoflurane inhalatory anesthesia (2.5% v/v) followed by IP injection of fentanyl (0.05 mg/kg) and re-opened by a midline sternotomy to perform intramyocardial transplantation (saline, 6×10^5 CD34⁺ cells or 1.2×10^6 MSC/animal in 5 injections of 5- μ l volume, at 5 points of the infarct border zone with a Hamilton syringe).

5-bromodeoxyuridine treatment and analysis of proliferating cells. After cell transplantation, each animal was given daily 0.5-ml IP injection of 5-bromodeoxyuridine (BrdU) (50 mg/kg body weight, IP) for 2 weeks. The BrdU was also given orally in tap water (1 mg/ml) (10). The BrdU-labeled cells in heart tissue were identified with an anti-BrdU antibody (Abcam, Cambridge, Massachusetts). Proliferation index was calculated as a percentage of BrdU-labeled nuclei/total of nuclei identified by 4'-6-diamidino-2-phenylantyl staining. Identification of proliferating myofibroblasts or cardiomyocytes was performed by double staining with anti-BrdU antibodies and anti-smooth muscle actin (SMA) or anti-troponin I, respectively (both antibodies from Chemicon International, Harrow, United Kingdom). One thousand SMA⁺ cells or troponin I⁺ cells were counted. The SMA⁺ cells incorporated into vessel structures were not included in the counting.

Functional assessment by echocardiography. Transthoracic echocardiography was performed in rats under inhalatory anesthesia (Sevoflurane) with an echocardiographic

Abbreviations and Acronyms

AW	= anterior wall thickness
BrdU	= 5-bromodeoxyuridine
EDA	= end-diastolic area
ESA	= end-systolic area
FAC	= fractional area change
FS	= fractional shortening
LV	= left ventricular
MI	= myocardial infarction
MSC	= mesenchymal stem cells
PW	= posterior wall thickness
SMA	= smooth muscle actin

Table 1 Echocardiographic Values of Saline-, CD34-, and MSC Groups

	Saline (n = 15)				CD34 ⁺ Cells (n = 11)				MSC (n = 14)			
	Baseline	MI	2 Weeks	4 Weeks	Baseline	MI	2 Weeks	4 Weeks	Baseline	MI	2 Weeks	4 Weeks
Awd	1.25 ± 0.06	0.93 ± 0.05	1.00 ± 0.05	0.99 ± 0.03	1.35 ± 0.08	1.28 ± 0.17	1.25 ± 0.09*	1.09 ± 0.08	1.12 ± 0.06	1.22 ± 0.12	1.07 ± 0.04	1.02 ± 0.06
Lvd	5.83 ± 0.12	6.76 ± 0.13	7.26 ± 0.20	7.47 ± 0.23†	5.78 ± 0.12	6.68 ± 0.16	7.08 ± 0.15	7.41 ± 0.19†	6.24 ± 0.12	7.29 ± 0.36	7.26 ± 0.18	7.44 ± 0.18
Pwd	1.25 ± 0.05	1.62 ± 0.22	1.31 ± 0.06	1.36 ± 0.09	1.45 ± 0.08	1.43 ± 0.14	1.57 ± 0.15	1.39 ± 0.13	1.40 ± 0.05	1.48 ± 0.06	2.16 ± .84	1.32 ± 0.06
AWs	2.19 ± 0.13	1.40 ± 0.12	1.35 ± 0.20	1.43 ± 0.10	2.30 ± 0.10	1.73 ± 0.20	1.97 ± 0.18†	1.71 ± 0.16	2.03 ± 0.10	1.75 ± 0.19	1.89 ± 0.10†	1.78 ± 0.08§
LVS	3.43 ± 0.12	4.95 ± 0.17	5.41 ± 0.25	5.67 ± 0.26†	3.42 ± 0.10	4.95 ± 0.18	4.90 ± 0.19	5.03 ± 0.18	3.64 ± 0.07	5.31 ± 0.37	4.97 ± 0.21	5.06 ± 0.19
PWs	1.99 ± 0.10	2.13 ± 0.09	2.03 ± 0.09	2.00 ± 0.12	2.15 ± 0.08	2.07 ± 0.18	2.08 ± 0.11	2.02 ± 0.12	1.93 ± 0.05	2.14 ± 0.10	2.02 ± 0.07	1.98 ± 0.05*
EDA	0.30 ± 0.01	0.36 ± 0.02	0.42 ± 0.01	0.43 ± 0.01†	0.29 ± 0.01	0.39 ± 0.02	0.41 ± 0.02	0.44 ± 0.02§	0.33 ± 0.01	0.41 ± 0.03	0.42 ± 0.02	0.43 ± 0.02
ESA	0.08 ± 0.01	0.21 ± 0.01	0.25 ± 0.01	0.27 ± 0.02†	0.07 ± 0.01	0.21 ± 0.02	0.20 ± 0.02*	0.23 ± 0.02	0.09 ± 0.01	0.23 ± 0.02	0.21 ± 0.01*	0.22 ± 0.02
FS	41.18 ± 1.85	26.89 ± 1.76	26.89 ± 1.76	26.00 ± 1.76	40.79 ± 1.56	26.13 ± 1.41	30.37 ± 1.69	32.17 ± 1.62†	41.49 ± 0.98	27.72 ± 1.87	31.77 ± 1.75*	32.07 ± 1.53
FAC	74.02 ± 1.36	41.61 ± 2.16	39.46 ± 1.79	38.00 ± 2.64	76.02 ± 1.91	45.51 ± 2.75	51.46 ± 3.02†	48.89 ± 2.41§	72.18 ± 1.28	43.43 ± 2.44	50.85 ± 1.66#	49.25 ± 2.16†§
AWT	41.90 ± 2.09	31.39 ± 2.62	24.95 ± 3.28	28.22 ± 3.27	41.16 ± 2.05	25.33 ± 3.32	34.13 ± 3.92	32.99 ± 4.83	45.03 ± 2.11	27.87 ± 5.22	40.91 ± 3.30†	41.35 ± 3.90

All values are mean ± SEM. Anterior wall diastole thickness (AWd), posterior wall diastole thickness (PWd), left ventricular diastole internal dimension (LVD), left ventricular systole internal dimension (LVS), and posterior wall systole thickness (PWS) are expressed in millimeters, whereas end-diastolic area (EDA) and end-systolic area (ESA) are expressed in millimeters squared. Fractional shortening (FS), fractional area change (FAC), and anterior wall thickening (AWT) are expressed as percentage. Significance values were calculated at 4 weeks (w) versus myocardial infarction (MI) in each group (†p < 0.05; ††p < 0.01). The p values among CD34 group and mesenchymal stem cells (MSC) group versus saline group were calculated at 2 weeks (*p < 0.05; †p < 0.01; ††p < 0.001) and 4 weeks (||p < 0.05; §p < 0.01).

system (General Electric, Waukesha, Wisconsin) equipped with a 10-MHz linear-array transducer as previously reported (7). Measurements were taken at baseline, after infarction, and after transplantation (2 weeks and 4 weeks). Left ventricular dimensions in end-diastole (LVDd) and end-systole (LVDs), anterior wall (AW) and posterior wall thickness in diastole and systole, end-diastolic area (EDA), and end-systolic area (ESA) were measured. Changes in AW were calculated as: $(AW_s - AW_d/AW_d) \times 100$. The FS was calculated as: $([LVDd - LVDs]/LVDd) \times 100$. Fractional area change (FAC) was calculated as: $([EDA - ESA]/EDA) \times 100$.

Immunohistochemistry and electron microscopy. Four weeks after implantation, animals were killed, and the hearts were removed and washed with phosphate-buffered saline and fixed in 2% paraformaldehyde or 2% paraformaldehyde/glutaraldehyde for electron microscopy examination. Heart tissue sections were prepared for immunohistochemistry as previously reported (7). For electron microscopy analysis, semi-thin (1.5 μ m) and ultrathin (0.05 μ m) sections were prepared (7). Muscular and fibrotic layer thickness at the infarct border were calculated in transmural LV wall semi-thin sections (n = 5 animals in each group), and values were

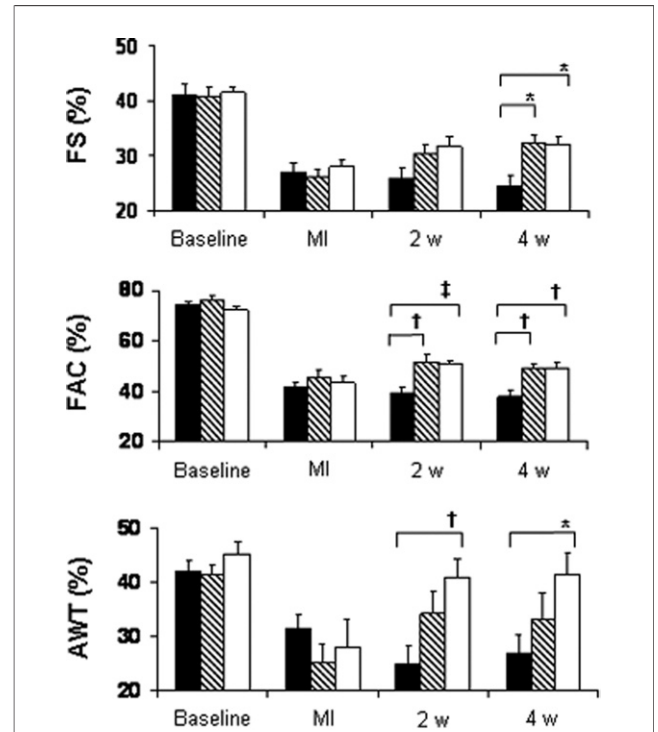


Figure 2 Measurement of LV Function in Saline-, CD34-, or MSC-Treated Animals

Measurement of left ventricular (LV) function in saline-treated (n = 15), CD34-treated (n = 11), or mesenchymal stem cells (MSC)-treated (n = 14) animals. Quantified values of fractional shortening (FS), fractional area change (FAC), and anterior wall thickening (AWT) are given. Saline group (solid bars), CD34 group (ruled bars), and MSC group (open bars). *p < 0.05; †p < 0.01; ††p < 0.001. MI = myocardial infarction.

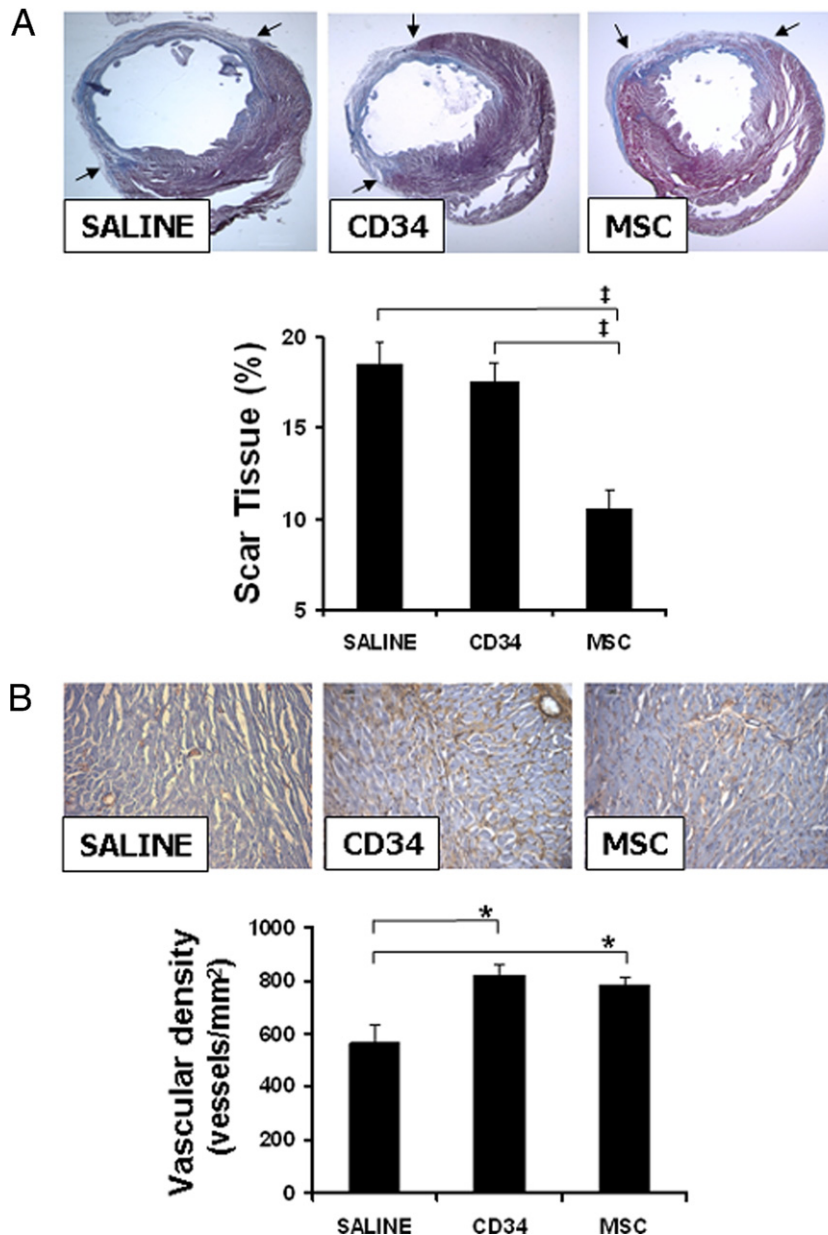


Figure 3 Effect of Cell Transplantation on Infarct Size

(A) Representative heart sections from infarcted nude rats receiving saline, CD34⁺ cells, or mesenchymal stem cells (MSC). Fibrotic area in the left ventricle was calculated in Masson's Trichrome stained sections. **Arrows** point to the border zones of the infarct. (B) Neovascularization in the border infarct, 4 weeks after cell transplantation. Representative sections and quantification of the total number of vessels in all groups (n = 6 in each group). *p < 0.05; †p < 0.001.

expressed as a percentage of the total LV wall thickness. Cellular infiltrates were identified on heart tissue after staining of paraffin-embedded sections with hematoxylin/eosin solution (Merk, Darmstadt, Germany).

Vascular density analysis. Immunohistochemical detection of vessels was performed with anti-rat CD31 (Chemicon International). Vessels were counted in 10 fields in the peri-infarct zone at 200 \times and referred as number of vessels/unit area (mm²) with a light microscope and the

Image Pro-Plus 5.1 software (Media Cybernetics, Inc., Bethesda, Maryland).

Morphometry. The infarct size in the LV was measured in 8 to 12 transverse sections of 14 μ m (1 slice each 200 μ m of tissue) from apex to base, fixed with 2% paraformaldehyde, and stained with Masson's trichrome. The fibrotic zone was determined by computer planimetry (Image Pro-Plus 5.1 software, Media Cybernetics, Inc.). Infarct size was expressed as percentage of total LV area and as a mean of all slices from each heart.

Terminal deoxynucleotidyl transferase dUTP nick end labeling assay. Apoptotic cells in heart tissue were detected with the ApopTagPlus Fluorescein In situ Apoptosis Detection Kit (Chemicon International) following the manufacturers' instructions.

Statistical analysis. Data are expressed as mean \pm SEM. All statistical analyses were performed with the SPSS software, version 14.0 (SPSS, Chicago, Illinois). Comparisons between MI and 4 weeks after transplantation in each group were performed with a Wilcoxon W test. Pairwise comparisons between groups at different time points were done with a Mann-Whitney U test. Differences were considered statistically significant at $p < 0.05$ with a 95% confidence interval.

Results

MSC and CD34⁺ cells isolation, characterization, and labeling. Purified CD34⁺ cells were labeled with CM-Di I (Molecular Probes), washed, and used for some in vivo studies. Percentage of labeled cells was more than 99.5% (Fig. 1A). Human bone marrow MSC were expanded, characterized, and labeled with green fluorescent protein by retroviral transduction (Fig. 1B). The percentage of infection was $90 \pm 5\%$. The MSC phenotype was maintained after retroviral labeling as determined by fluorescein-activated cell sorting analysis (Fig. 1B).

Cell transplantation and LV function. Seven days after MI, 6×10^5 CD34⁺ cells or 1.2×10^6 MSC were injected intramyocardially. The optimal doses to induce improvement in cardiac function were selected on the basis of previous studies performed by our group and others (7,11). Because CD34⁺ cells display a higher proliferative capacity in vitro and in vivo, we inoculated half dose with respect to MSC. Furthermore, the dose used for CD34⁺ cells was sufficient to improve cardiac function as described (11). The echocardiographic parameters from all groups are listed in Table 1. Changes were monitored at baseline, after MI, and after transplantation (2 and 4 weeks). At baseline and after MI, the values of the echocardiographic parameters analyzed were similar among the 3 groups, indicating comparable levels of tissue injury. In cell-treated groups, the improvement in cardiac performance in terms of FS and FAC was observed 2 weeks after transplantation and maintained at least 2 more weeks (Fig. 2). Indeed, 4 weeks after transplantation, FAC was $38.00 \pm 2.64\%$ in saline, $48.89 \pm 2.41\%$ in the CD34 group, and $49.25 \pm 2.16\%$ in the MSC group ($p < 0.01$ in CD34 and MSC vs. saline). At this time point, FS was $26.00 \pm 1.76\%$ in saline, $32.17 \pm 1.62\%$ in the CD34 group, and $32.07 \pm 1.53\%$ in the MSC group ($p < 0.05$ in CD34 and MSC vs. saline). The AW thickening was significantly higher in animals transplanted with MSC ($28.22 \pm 3.27\%$ in saline, $32.99 \pm 4.83\%$ in the CD34 group, and $41.35 \pm 3.90\%$ in the MSC group; $p < 0.05$ in MSC vs. saline at 4 weeks), indicating that MSC

were more effective in preventing wall thinning and remodeling than CD34⁺ cells (Fig. 2).

Wall thickness and angiogenesis in CD34 and MSC transplanted animals. Quantification of infarct area in animals from each group revealed that only the MSC group showed a reduced area of fibrous scar tissue (Fig. 3A). Percentage of scar tissue was $18.49 \pm 1.58\%$ in the saline group, $17.48 \pm 1.29\%$ in the CD34 group, and $10.36 \pm 1.07\%$ in the MSC group ($p < 0.001$ in MSC vs. saline and CD34). Capillary density in the LV wall was significantly greater in the CD34 and MSC groups than in the saline group, as assessed 28 days after implantation (Fig. 3B). Number of vessels/mm² were 567 ± 63 in the saline group, 818 ± 41 in the CD34 group, and 781 ± 35 in the MSC group ($p < 0.05$ in CD34 vs. saline and MSC vs. saline), confirming the strong ability of MSC and CD34⁺ cells to induce neoangiogenesis.

Organization of the infarcted tissue in CD34 and MSC groups. Analysis of ultrathin sections from infarct border tissue revealed the marked thinning of ventricular wall in the saline group, due to the fibrotic scar maturation, 4 weeks after treatment (Fig. 4). In contrast, in the CD34 and MSC

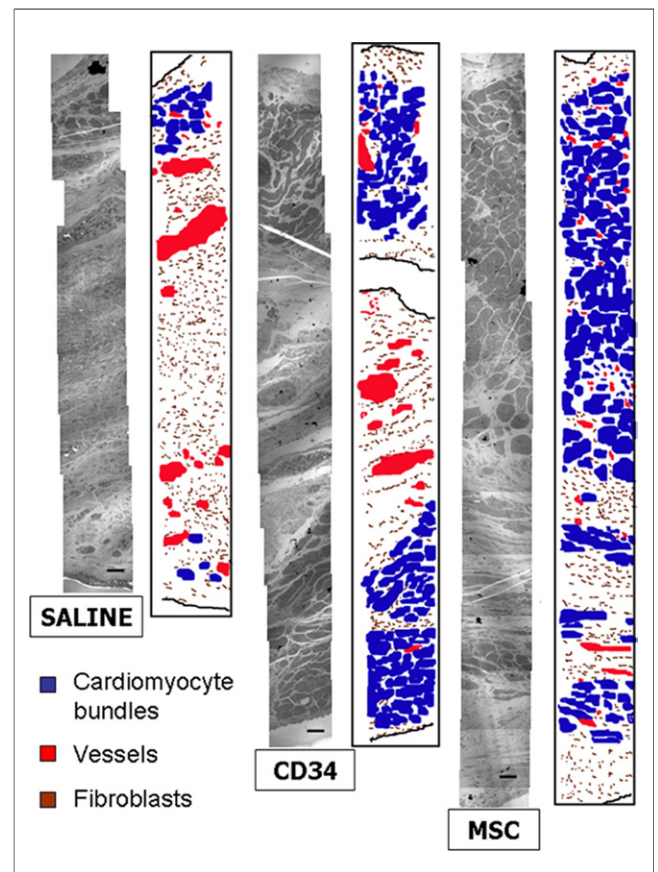


Figure 4 Organization of Cardiac Tissue at the Peri-Infarct Zone

Representative ultra-thin sections of left ventricular walls at the peri-infarct zone from a control-, CD34-, or mesenchymal stem cells (MSC)-transplanted animal, 4 weeks after transplantation. Contiguous electron micrographs were assembled into a photomontage. The contours of the different cell types were traced in different colors. Scale bar = 5 μm .

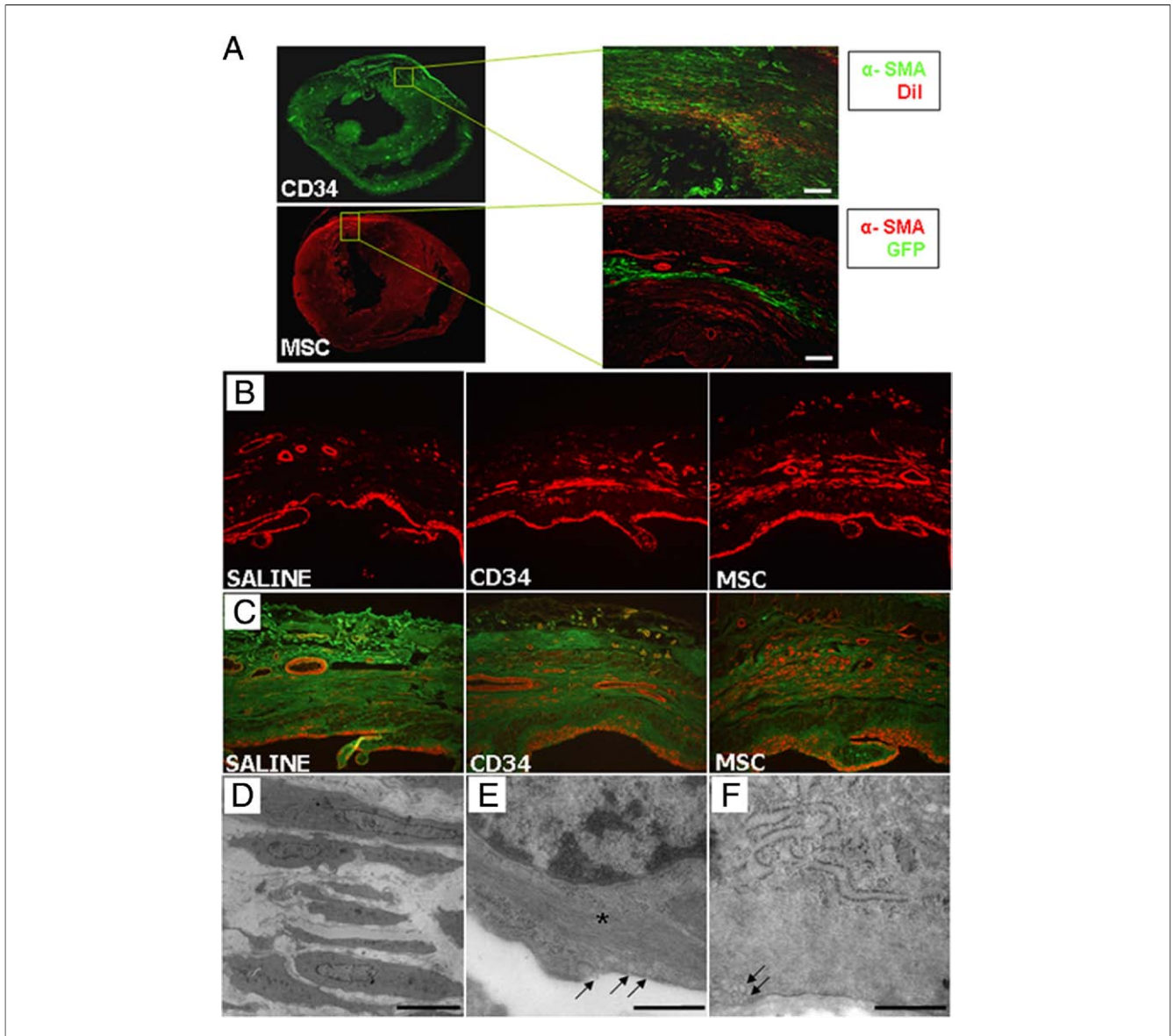


Figure 5 Localization of CD34 or MSC-Transplanted Cells in the Border and Infarct Zone

(A) Heart sections of CD34- and MSC-transplanted animals, respectively. Areas included in the squares are shown at higher magnification on the left of the figure. To visualize human transplanted cells, in CD34-transplanted animals, cells were labeled with Dil (red) and fibrotic tissue was stained in green with anti-smooth muscle actin (SMA) antibodies, whereas in MSC-treated animals, MSC retrovirally labeled with GFP were visualized by the green epifluorescence, and tissue was labeled in red with anti-SMA antibodies. (B) Immunohistochemistry of infarcted heart sections from different groups with anti-rat SMA antibodies. (C) Double immunostaining with anti-SMA (red) and anti-collagen I (green). (D) Myofibroblast rim detection by electron microscopy. (E) Detail of myofiber organization in a myofibroblast. (F) Ultrastructural detail of a fibroblast. *Myofiber bundles along the cell axis. Arrows show vesicles of exocytosis. Scale bar = 100 μ m in A, 5 μ m in D, and 0.5 μ m in E and F. (B, C = 100 \times magnification). Other abbreviations as in Figure 1.

groups, animals showed an enlargement of subepicardium and subendocardium cardiomyocyte layers at the same time point. Moreover, the MSC group showed additional bands of myocardial tissue disposed between the fibrotic layers, resulting in further increase of LV wall thickness. Cardiomyocyte muscle layers at the infarct border constituted $45.16 \pm 7.23\%$ of the total LV wall thickness in the saline group, $48.41 \pm 7.59\%$ in the CD34 group, and $71.0 \pm 2.39\%$ in the MSC group ($p < 0.05$ in MSC vs. CD34 and vs. saline). A comparison between MSC and CD34⁺ cells

migratory capacity in ischemic tissue showed that most CD34⁺ cells were retained at the site of injection, whereas MSC migrate from the site of implantation to the infarcted zone and were placed in the intermediate fibrotic rim between subepicardium and subendocardium ($n = 4$) (Fig. 5A). Interestingly, in this layer we observed differences in infarcted tissue organization among groups. The MSC group showed an increase in myofibroblast, as detected by anti-SMA. This myofibroblast layer was thinner in the CD34 group and nearly absent in the saline group (Fig 5B). On the contrary,

expression of collagen I at the infarct zone was reduced in the MSC group but not in the CD34 group (Fig. 5C), indicating the influence of MSC transplantation in extracellular matrix reorganization. Because there is paucity in antibodies able to distinguish myofibroblasts from fibroblasts, electron microscopy analysis was performed to further characterize the fibroblast/myofibroblasts rim (Fig. 5D). Although identical in size, shape, and cytoplasmic structure, myofibroblasts were distinguished from fibroblasts by the presence of abundant myofilaments along the cellular axis (Figs. 5E and 5F). The fact that the MSC group showed increased

myofibroblast accumulation and decreased collagen deposition correlated with morphometric studies and pointed to the superior ability of MSC to inverse LV remodelling.

Tissue regeneration in stem cell-treated animals. To investigate whether anterior wall thickening and decrease of infarct size was associated with cell proliferation in infarcted tissue, we quantified the number of BrdU⁺ cells in the LV of BrdU-treated animals (n = 5 in each group). The results showed that MSC induced the highest cell proliferation in myocardial tissue (proliferation index was 12.3 ± 1.5% in the saline group, 17.3 ± 2.5% in the

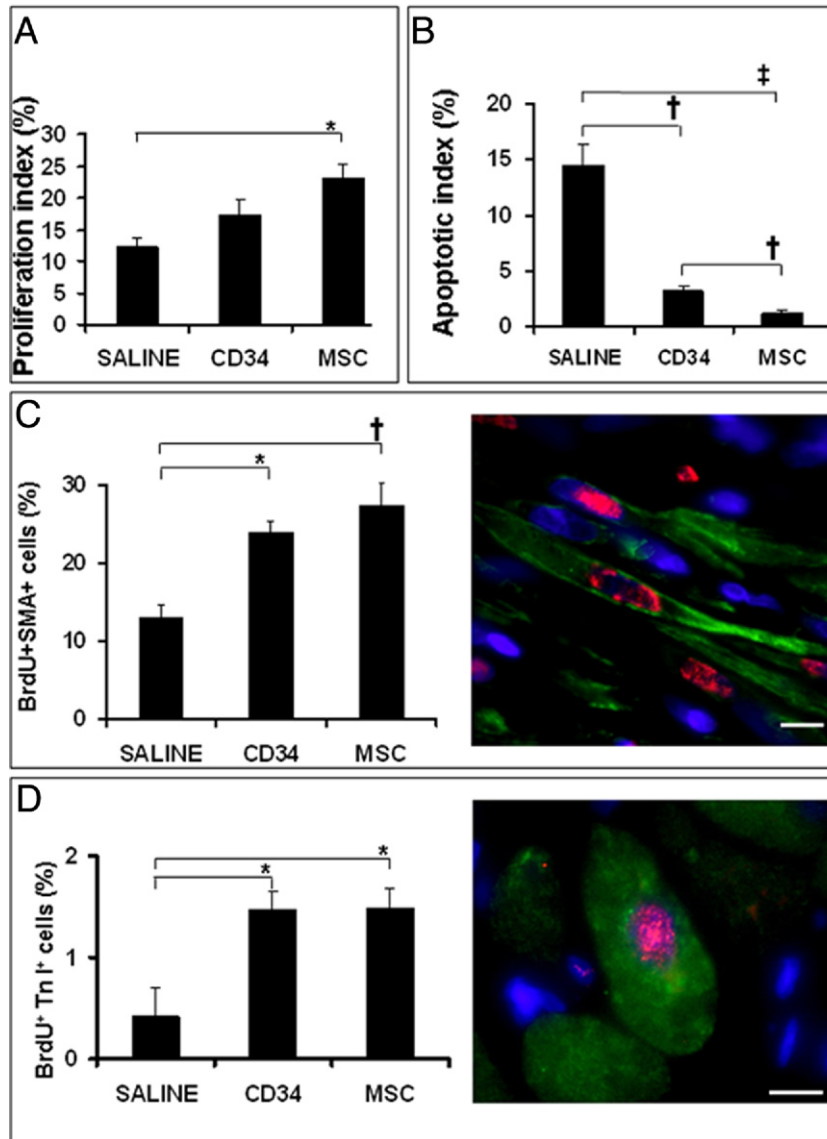


Figure 6 Analysis of Tissue Regeneration in Stem Cell-Treated Animals

(A) Total number of 5-bromodeoxyuridine (BrdU⁺) cells. (B) Percentage of apoptotic cells assessed by terminal deoxynucleotidyl transferase dUTP nick end labeling assay. (C, D) Percentage of proliferating smooth muscle actin (SMA)⁺ cells and cardiomyocytes, as detected by double staining with anti-BrdU (pink) and anti-SMA (green) or anti-Troponin (Tn) I (green) antibodies, respectively. Representative images of double staining are shown. Nuclei were stained with 4'-6-diamidino-2-phenylindole. Scale bar = 5 μm. Results are expressed as mean ± SEM (%) (n = 5 in each group). *p < 0.05; †p < 0.01; ‡p < 0.001.

CD34 group, and $23.2 \pm 2.2\%$ in the MSC group; $p < 0.05$ in MSC vs. saline) (Fig. 6A). In addition, the number of apoptotic cells in the border zone of animals transplanted with MSC was lower than in the other groups (14.43 ± 1.87 in the saline group, 3.20 ± 0.40 in the CD34 group, and 1.20 ± 0.30 in the MSC group; $p < 0.01$ in CD34 vs. saline and MSC vs. saline) (Fig. 6B). A more exhaustive analysis revealed that most BrdU⁺ cells showed a fibroblastic morphology and were positively stained with anti-rat SMA antibodies (proliferation index of SMA⁺ cells was $12.93 \pm 1.64\%$ in the control group, $23.81 \pm 1.53\%$ in the CD34 group, and $27.36 \pm 2.88\%$ in the MSC group; $p < 0.05$ in CD34 vs. saline and $p < 0.01$ in MSC vs. saline) (Fig. 6C). Interestingly, troponin I staining revealed the presence of proliferating cardiomyocytes (cardiomyocyte proliferation index was $0.42 \pm 0.28\%$ in the control group, $1.49 \pm 0.20\%$ in the CD34 group, and $1.59 \pm 0.18\%$ in the MSC group; $p < 0.05$ in CD34 vs. saline and MSC vs. saline) (Fig. 6D). These

proliferating cells were not from human origin, because they were not stained with anti-human nuclei antibodies (not shown). Thus they might be a consequence of paracrine effects exerted by transplanted cells.

Collateral effects induced by stem cell transplantation. It is known that cell transplantation promotes interstitial mononuclear cell infiltration shortly after infusion. However, CD34-treated animals showed higher levels of cell infiltration in comparison with MSC transplanted animals at the latest time points (Fig. 7A). This effect was markedly patent in the epicardial tissue where animals from the CD34 group showed dramatic cell infiltration in comparison with MSC and saline groups (Fig. 7B).

Discussion

Adult stem cell transplantation is an adjuvant treatment to conventional therapies of cardiac ischemic injury. However, the best cell type for each therapeutic application remains to be determined, and more preclinical studies should be

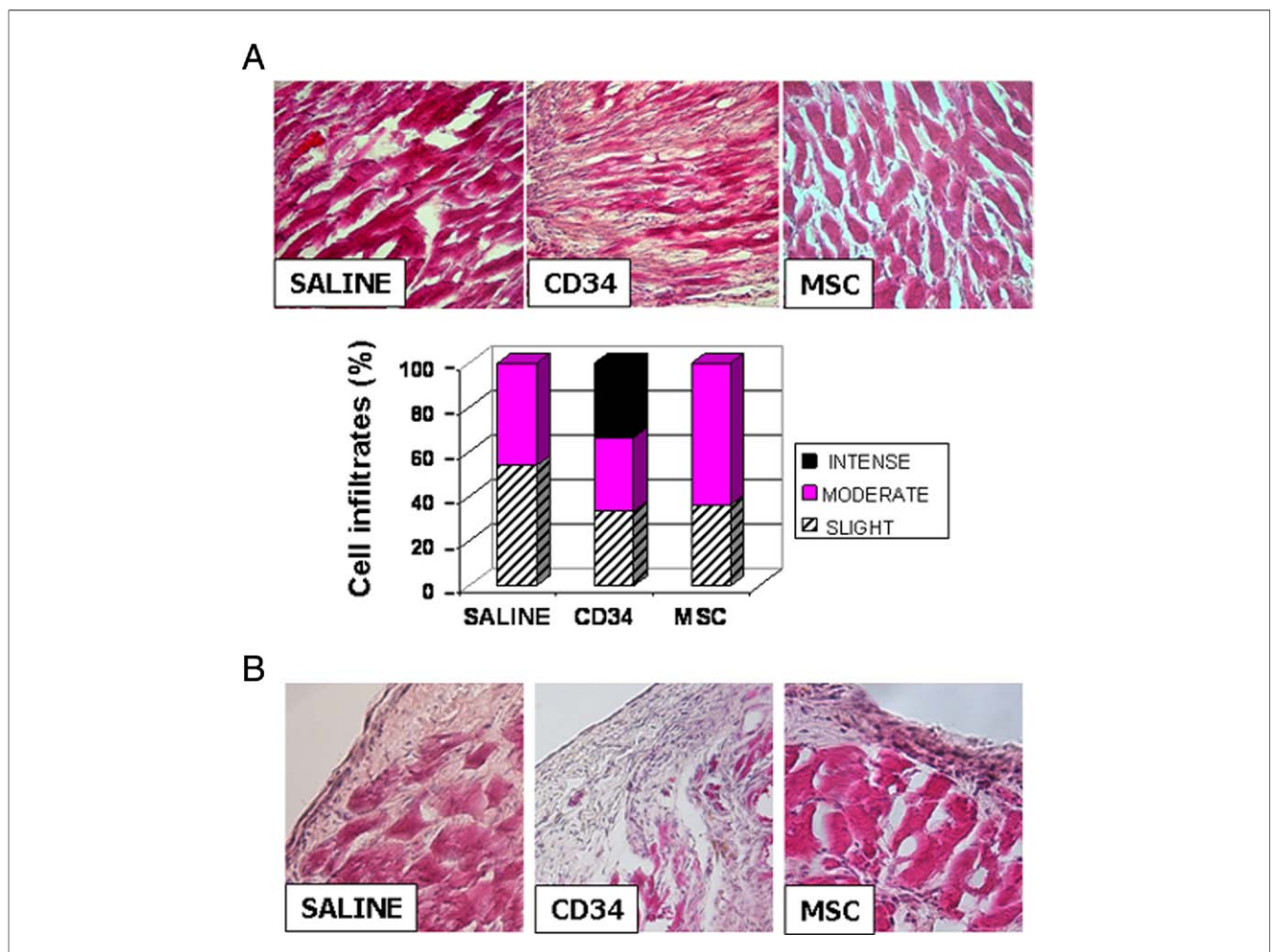


Figure 7 Analysis of Cell Infiltration in Stem Cell-Treated Animals

(A) Quantification of infiltrating cells in saline-, CD34-, and mesenchymal stem cells (MSC)-treated animals classified as slight, moderate, or intense. **(B)** Detail of epicardial tissue in representative sections of saline, CD34, and MSC transplanted animals (100× magnification).

performed to define the most suitable cell type to be used in the clinical practice (3,12,13).

In this study we demonstrate that MSC transplantation prevents ventricular remodelling and exerts fewer collateral effects than CD34⁺ cell transplantation. We did not find significant differences in ventricular performance between MSC and CD34 groups in terms of FS and FAC at 2 or 4 weeks after transplantation. However, echocardiographic parameters related to wall thickening and morphometric/histological studies clearly showed that MSC transplantation prevented the thinning of the LV wall and decreased infarct size more efficiently than CD34⁺ cell transplantation. The higher sensibility of histological and electron microscopy versus echocardiography to evaluate myocardial architecture and heart geometry in small animals could explain these discrepancies.

General consensus supports the paracrine hypothesis to explain cardiac repair (14–16). The superior ability of MSC to migrate from the site of injection to the infarcted zone, in comparison with CD34⁺ cells, could help them to exert their paracrine effect. Indeed, hypoxia or inflammatory mediators in the ischemic niche could be responsible for MSC migration. For instance, hypoxia induces CXCR4 upregulation via hypoxia inducible factor-1- α (17), and a recent work shows that stromal cell-derived factor-1- α /CXCR4 interaction is involved in the retention of MSC in the ischemic heart (18). In a similar way, tumor necrosis factor- α pre-treatment or overexpression enhances MSC engraftment in cardiac tissue and improves recovery of cardiac function after MI (13,19).

Other phenomena could explain the differences in the wound-healing process observed among groups. MSC transplantation favors myofibroblast proliferation as observed in BrdU experiments. In addition, the myofibroblast middle layer was thicker in animals transplanted with both stem cell types than in the saline group but more markedly in the MSC group, as detected by immunohistochemistry with anti-SMA⁺ antibodies. Myofibroblasts confer elasticity and contractility to the LV wall and improve wall motion and healing (20,21). After MI, myofibroblasts proliferate to promote infarct healing but die a few days later when the scar is generated in the infarcted region (22). Thus, therapies capable of activating this cell type would be beneficial in the wound repair (22,23).

Another important observation is the ability of MSC to reduce collagen I deposition at the infarct zone. Although we could not quantify it, previous works have shown the influence of MSC transplantation in attenuation of fibrosis and collagen I deposition (24–26).

Conclusions

We have demonstrated that CD34⁺ cells—their therapeutic potential notwithstanding—induce a chronic cell infiltration

of cardiac tissue and do not efficiently prevent LV remodelling. Mesenchymal stem cells, however, migrate to the site of infarction, potentiate the healing of the infarct, and control the remodelling process. Thus, the latter seems to be more appropriate to use in clinical practice for the treatment of MI.

Acknowledgments

The authors are indebted to Dr. A. Chapel for the gift of the pSF-G13 cell line. The authors thank A. Hernández and E. Lafuente from the Service of Confocal microscopy at Centro de Investigación Príncipe Felipe for technical assistance, and M. Llop and M. Soriano for electron microscopy micrographs.

Reprint requests and correspondence: Dr. Pilar Sepúlveda, Fundación para la Investigación Hospital Universitario La Fe, Regenerative Medicine and Heart Transplantation Unit, Avda Campanar 21, Valencia 46009, Spain. E-mail: pilar.sepulveda@uv.es. OR Dr. J. Anastasio Montero, Hospital Universitario La Fe, Servicio de Cirugía Cardíaca, Avda Campanar 21, Valencia 46009, Spain. E-mail: montero_jos@gva.es.

REFERENCES

1. Strauer BE, Brehm M, Zeus T, et al. Repair of infarcted myocardium by autologous intracoronary mononuclear bone marrow cell transplantation in humans. *Circulation* 2002;106:1913–8.
2. Schachinger V, Erbs S, Elsasser A, et al. Intracoronary bone marrow-derived progenitor cells in acute myocardial infarction. *N Engl J Med* 2006;355:1210–21.
3. Dimmeler S, Zheider AM, Schneider MD. Unchain my heart: the scientific foundations of cardiac repair. *J Clin Invest* 2005;115:572–83.
4. Bartunek J, Vanderheyden M, Vandekerckhove B, et al. Intracoronary injection of CD133-positive enriched bone marrow progenitor cells promotes cardiac recovery after recent myocardial infarction: feasibility and safety. *Circulation* 2005;112:1178–83.
5. Chen S, Liu Z, Tian N, et al. Intracoronary transplantation of autologous bone marrow mesenchymal stem cells for ischemic cardiomyopathy due to isolated chronic occluded left anterior descending artery. *J Invasive Cardiol* 2006;18:552–6.
6. Giordano A, Galderisi U, Marino IR. From the laboratory bench to the patient's bedside: an update on clinical trials with mesenchymal stem cells. *J Cell Physiol* 2007;211:27–35.
7. Gandia C, Arminan A, Garcia-Verdugo JM, et al. Human dental pulp stem cells improve left ventricular function, induce angiogenesis and reduce infarct size in rats with acute myocardial infarction. *Stem Cells* 2008;26:638–45.
8. Sepúlveda P, Encabo A, Carbonell-Uberos F, Minana MD. BCL-2 expression is mainly regulated by JAK/STAT3 pathway in human CD34⁺ hematopoietic cells. *Cell Death Differ* 2007;14:378–80.
9. Friedrich J, Apstein CS, Ingwall JS. 31P nuclear magnetic resonance spectroscopic imaging of regions of remodeled myocardium in the infarcted rat heart. *Circulation* 1995;92:3527–38.
10. Rota M, Padin-Iruegas ME, Misao Y, et al. Local activation or implantation of cardiac progenitor cells rescues scarred infarcted myocardium improving cardiac function. *Circ Res* 2008;103:107–16.
11. Iwasaki H, Kawamoto A, Ishikawa M, et al. Dose-dependent contribution of CD34-positive cell transplantation to concurrent vasculogenesis and cardiomyogenesis for functional regenerative recovery after myocardial infarction. *Circulation* 2006;113:1311–25.

12. Smart N, Riley PR. The stem cell movement. *Circ Res* 2008;102:1155–68.
13. Behfar A, Faustino RS, Arrell DK, Dzeja PP, Perez-Terzic C, Terzic A. Guided stem cell cardiopoiesis: discovery and translation. *Journal of molecular and cellular cardiology* 2008;45:523–9.
14. Gnechi M, Zhang Z, Ni A, Dzau VJ. Paracrine mechanisms in adult stem cell signaling and therapy. *Circ Res* 2008;103:1204–19.
15. Mangi AA, Noiseux N, Kong D, et al. Mesenchymal stem cells modified with Akt prevent remodeling and restore performance of infarcted hearts. *Nat Med* 2003;9:1195–201.
16. Rubart M, Field LJ. Cell-based approaches for cardiac repair. *Ann N Y Acad Sci* 2006;1080:34–48.
17. Schioppa T, Uranchimeg B, Saccani A, et al. Regulation of the chemokine receptor CXCR4 by hypoxia. *J Exp Med* 2003;198:1391–402.
18. Zhang D, Fang G, Zhou X, et al. Over-expression of CXCR4 on mesenchymal stem cells augment myoangiogenesis in infarcted myocardium. *J Moll Cell Cardiol* 2008;44:281–92.
19. Kim YS, Park HJ, Hong MH, et al. TNF-alpha enhances engraftment of mesenchymal stem cells into infarcted myocardium. *Front Biosci* 2009;14:2845–56.
20. Tomasek JJ, Gabbiani G, Hinz B, Chaponnier C, Brown RA. Myofibroblasts and mechano-regulation of connective tissue remodeling. *Nat Rev Mol Cell Biol* 2002;3:349–63.
21. van Amerongen MJ, Bou-Gharios G, Popa ER, et al. Bone-marrow derived myofibroblasts contribute functionally to scar formation after myocardial infarction. *J Pathol* 2008;214:377–86.
22. Hayakawa K, Takemura G, Kanoh M, et al. Inhibition of granulation tissue cell apoptosis during the subacute stage of myocardial infarction improves cardiac remodeling and dysfunction at the chronic stage. *Circulation* 2003;108:104–9.
23. Virag JI, Murry CE. Myofibroblast and endothelial cell proliferation during murine myocardial infarct repair. *Am J Pathol* 2003;163:2433–40.
24. Li L, Zhang Y, Li Y, et al. Mesenchymal stem cell transplantation attenuates cardiac fibrosis associated with isoproterenol-induced global heart failure. *Transpl Int* 2008;21:1181–9.
25. Ohnishi S, Sumiyoshi H, Kitamura S, Nagaya N. Mesenchymal stem cells attenuate cardiac fibroblast proliferation and collagen synthesis through paracrine actions. *FEBS Lett* 2007;581:3961–6.
26. Yokokawa M, Ohnishi S, Ishibashi-Ueda H, et al. Transplantation of mesenchymal stem cells improves atrioventricular conduction in a rat model of complete atrioventricular block. *Cell Transplant* 2008;17:1145–55.

Key Words: hematopoietic precursors ■ left ventricular function ■ mesenchymal stem cells ■ myocardial infarction ■ paracrine factors.